

Design goals for Hall D replacement solenoid

G. BIALLAS, E. CHUDAKOV, E.S. SMITH, T. WHITLATCH, E. WOLIN

1 Background

The equipment in Hall D for use in the 12 GeV program at Jefferson Lab is based on a solenoidal magnet, which was first used at SLAC for the LASS experiment and then later at Los Alamos for the MEGA experiment. Jefferson Lab is investigating the possibility of building a modern magnet which could be used to replace this aging solenoid. The current magnet provides a 2.2 T magnetic field parallel to the beam direction at the center of the magnet. The inside diameter of the magnet is 185 cm and its overall length is 465 cm. In the configuration for Hall D, the inductance of the coil is 26.2 H, and the magnet will run at a nominal current of 1500 A resulting in a stored energy of 29.5 MJ. The magnet in its original configuration and use at SLAC are described in the technical note of Ref. [1]. Modifications and properties of the magnet configuration, which will be used in Hall D, are summarized in Ref. [2]. We will refer to this solenoid as the “LASS” magnet.

The solenoid is constructed of four separate superconducting toroidal coils and cryostats. A 306 ton iron flux return path, similarly split in four places surrounds and supports the coil assemblies. A common liquid helium reservoir is located atop the solenoid providing the gravity feed of the liquid to the coils. Full access to the interior is provided from both ends of the magnet for installation and maintenance of detectors.

2 Scope

This document gives the design goals for a new solenoidal magnet to be used for experiments in Hall D at Jefferson Lab. The intent is to provide sufficient information that a design for such a magnet can be developed. The experimental equipment has been designed around the LASS magnet, and considerable infrastructure is in place to support the magnet operation. We assume that the yoke steel will be reused, which defines a geometry compatible with the Hall D detector. Several interfaces, indicated below, can be reused to facilitate integration of the new magnet, but should not be considered fixed constraints if they limit its design or fabrication. A sketch of the magnet, yoke and Hall D detectors are shown in Fig. 1 with a calculated magnetic field for a symmetric coil arrangement superimposed. The interface drawing (Drawing D00000-04-02-3000) should be used to obtain dimensions and specific constraints. For convenience, we define a cylindrical coordinate system with the z along the axis of the solenoid and $z=0$ defined by the downstream edge of the upstream yoke end-piece.

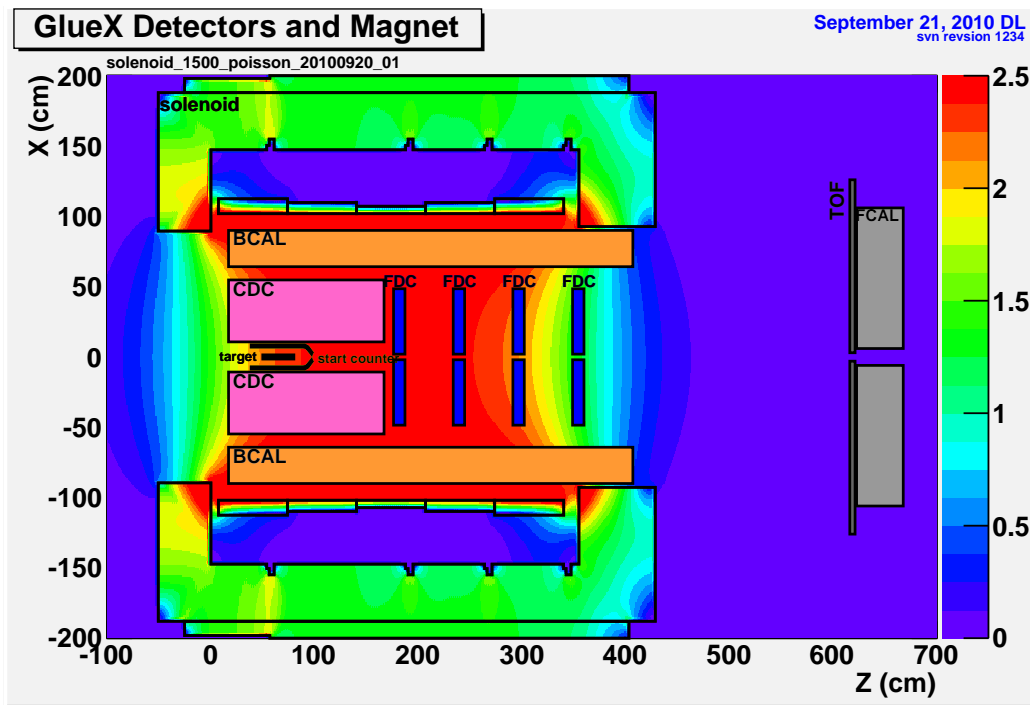


Figure 1: Cross sectional view of the solenoidal magnet and Hall D detector. The location of detectors relative to the magnet is shown. Included are the yoke steel and a concept for a single coil with increased number of Amp-turns at the ends, which provides a relatively uniform magnetic field in the tracking region. The color ramp is the magnetic field magnitude in Tesla.

The variable r is the radial distance from the z axis. The experimental target is a 30-cm-long cylinder parallel to z and centered on ($z=65$ cm, $r=0$ cm).

3 Magnetic field

3.1 Tracking volume

The magnetic field serves both to channel electromagnetic background downstream along the beamline and to bend charged particles in the magnetic field so that particle trajectories originating in the experimental target can be reconstructed with sufficient momentum resolution ($\sim 1-3\%$) to satisfy the experimental program. The sensitive tracking volume contains the drift chambers and is defined by $17 \leq z \leq 360$ cm and $r \leq 65$ cm. The magnetic field in this volume must be within the limits given in Table 1. These limits are displayed graphically in Figs. 2–4. The z -component of the magnetic field, B_z , is required to be between the upper and lower curves in Fig. 2. The asymmetric field of the LASS magnet is a good match to our experimental program. The high magnetic field at large z is required both to achieve the necessary resolution and to minimize electromagnetic background hits in the detectors. For small z , high

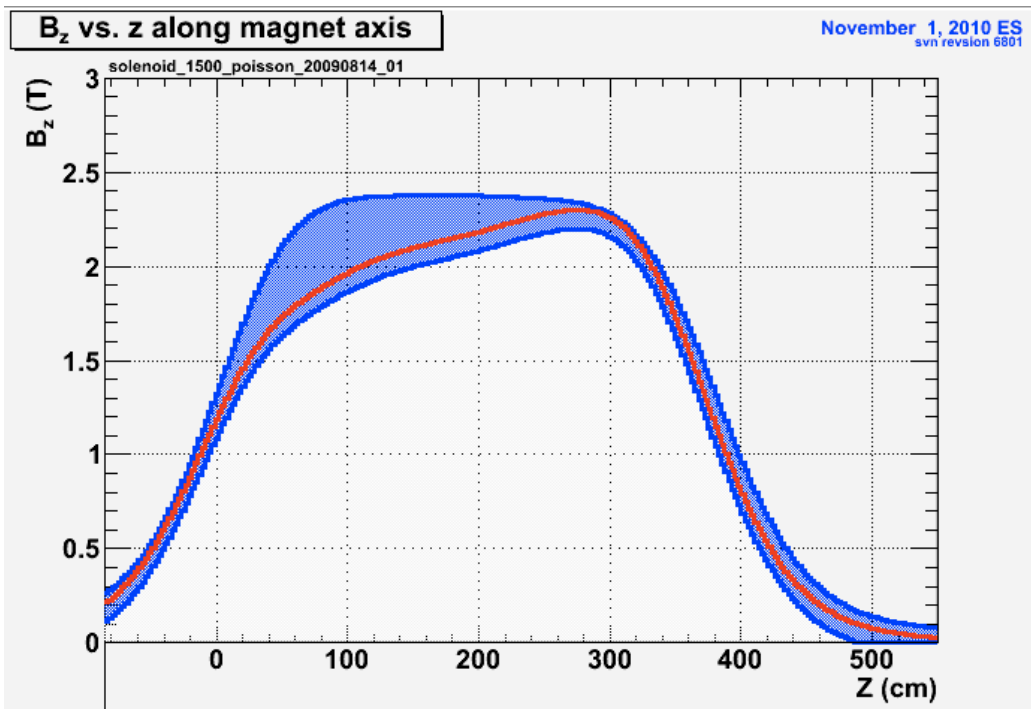


Figure 2: The allowed range of $B_z(z, r = 0)$ as a function of z is shown in blue. The curve in red shows the field for the LASS magnet, which indicates the preference of the experiment.

fields reduce acceptance of low-energy particles, so only moderate field strength is desirable or required. Therefore, although a rather large range of B_z is acceptable, the experiment has a preference for the minimum values of the allowed range. The symmetric fields could reduce local stresses and therefore reduce costs by facilitating the construction of the coil. The maximum variations of $B(r)$ occur at the largest radii, and therefore the allowance for changes from the central field are highest for $r=65$ cm, which are shown as a function of z in Figs. 3 and 4.

3.2 Fringe field

For proper operation of the photomultiplier tubes for the time-of-flight scintillators and the forward calorimeter, the fields must be limited in this region. The fringe field for $z \geq 600$ cm and $r \geq 10$ cm must be kept below 150 G.

4 Interfaces

The new magnet is required to be compatible with the Hall D detector and the yoke defines a geometry that minimizes potential conflicts. In addition, there is substantial infrastructure to support the operation of the LASS magnet, and these services and interfaces are available for reuse with the replacement magnet. These materials and

| z (cm) | Min $B_z(0)$ (T) | Max $B_z(0)$ (T) | $\frac{ B_z(65) - B_z(0) }{ B_z(0) }$ | $\frac{ B_r(65) - B_r(0) }{ B_z(0) }$ |
|-------------|---------------------|---------------------|---------------------------------------|---------------------------------------|
| -76 | 0.16 | 0.31 | | |
| -51 | 0.38 | 0.52 | | |
| -25 | 0.70 | 0.86 | | |
| 0 | 1.09 | 1.32 | 0.22 | 0.65 |
| 25 | 1.42 | 1.78 | 0.26 | 0.31 |
| 51 | 1.63 | 2.11 | 0.16 | 0.14 |
| 76 | 1.77 | 2.29 | 0.09 | 0.09 |
| 102 | 1.87 | 2.35 | 0.05 | 0.10 |
| 127 | 1.95 | 2.37 | 0.04 | 0.09 |
| 152 | 2.00 | 2.38 | 0.05 | 0.10 |
| 178 | 2.04 | 2.38 | 0.05 | 0.10 |
| 203 | 2.09 | 2.37 | 0.05 | 0.10 |
| 229 | 2.14 | 2.37 | 0.04 | 0.10 |
| 254 | 2.18 | 2.36 | 0.06 | 0.10 |
| 279 | 2.20 | 2.33 | 0.10 | 0.11 |
| 305 | 2.14 | 2.26 | 0.18 | 0.18 |
| 330 | 1.92 | 2.08 | 0.25 | 0.39 |
| 356 | 1.53 | 1.75 | 0.16 | 0.72 |
| 381 | 1.05 | 1.31 | | |
| 406 | 0.61 | 0.87 | | |
| 432 | 0.30 | 0.53 | | |
| 457 | 0.12 | 0.31 | | |
| 483 | 0.02 | 0.19 | | |
| 508 | 0.00 | 0.12 | | |
| 533 | 0.00 | 0.09 | | |
| 559 | 0.00 | 0.07 | | |
| 584 | 0.00 | 0.06 | | |

Table 1: Limits of components of the magnetic field. The limits on the radial dependence are only specified in the tracking volume. For $z \geq 600$ cm and $r \geq 10$ cm, the fringe field must be kept below 150 G.

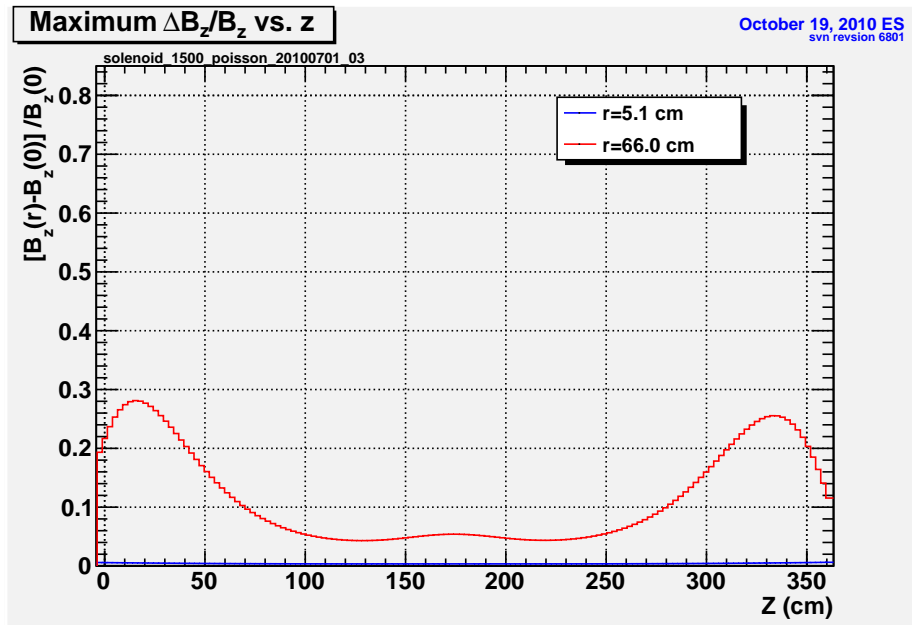


Figure 3: Maximum allowed fractional difference of $[B_z(r) - B_z(0)]/B_z(0)$ at small and large radial distances from the center within the tracking volume.

services are listed below, and their use will ease the integration of the magnet into the experiment. However, alternative equipment will be considered if it facilitates the design or fabrication of the new magnet.

4.1 Mechanical

There are several geometrical, or mechanical, constraints which need to be obeyed. The specific dimensions are given on the interface Drawing D00000-04-02-3000.

Yoke geometry. The yoke size determines the main dimensions of the magnet. The coil will be supported by the yoke. All cryogenic connections must come through the openings in the yoke. The yoke has four vertical shafts and four horizontal openings for cryogenic connections and vacuum ports, two for each coil. These accesses are available for connections to the new magnet.

Space for coils. The space for the new coil will be slightly reduced relative to that for the four LASS coils, as shown in the drawing.

Support of barrel calorimeter. The space inside the coil must be kept clear for structure to hold the barrel calorimeter. A new single coil will prevent the use of the existing scheme to support the barrel calorimeter, which uses the space between coil cryostats. Therefore, radial space is reserved between the calorimeter and the new coil for detector support structure.

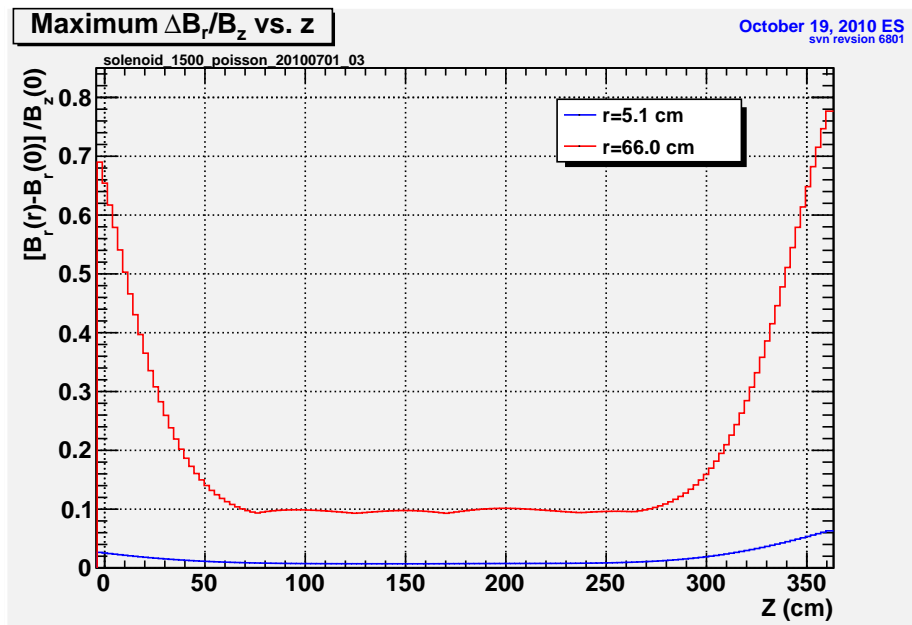


Figure 4: Maximum allowed fractional difference of $[B_r(r) - B_r(0)]/B_z(0)$ at small and large radial distances from the center within the tracking volume.

4.2 Cryogenics

Any solution compatible with the JLab cryogenic system is acceptable, but the existing cryogenic services are available and may be customized for use with the new coils. The access to the coil is through any or all of the four the openings in the yoke. The refrigeration for the LASS magnet is provided by a CTI Cryogenics Model 2800 4.5 K helium refrigerator, which can deliver a linear mix of up to 200 W of refrigeration or 2 g/s liquefaction. The cryogens are provided to a liquid helium reservoir, common to all four coils, located on top the solenoid, which then distributes He and LN₂ to each of the four individual LASS coils. Drawings of the system can be provided.

4.3 Power supply

The LASS solenoid is powered by a new Danfysik System 8000 Type 854 3000A, 10V DC power supply, which includes a quench detection circuit and energy dump system.

4.4 Magnet controls

The current magnet control system is based on the Allen-Bradley ControlLogix PLC family. It is modular, flexible and easily reconfigured and reprogrammed. Most of the instrumentation and programming is related to the cryogenic supply system and magnet power supply, which likely would be reused if the coil is replaced. The small fraction related to the superconducting magnet itself should easily be modified for a replacement coil.

4.5 Conductor

Jlab has available sufficient superconductor to fabricate a soldered composite conductor for the solenoidal coil. This superconductor can be made available to the vendor, but should not be taken as a requirement for the design or fabrication. The superconducting cable is comprised of 36 strands fabricated into a Rutherford style cable with a 1.01° keystone as shown in Fig. 5a. Typical dimensions of a composite cable conductor and insulation are also shown in the figure, but the vendor would propose a conductor and stabilizer that optimizes their design.

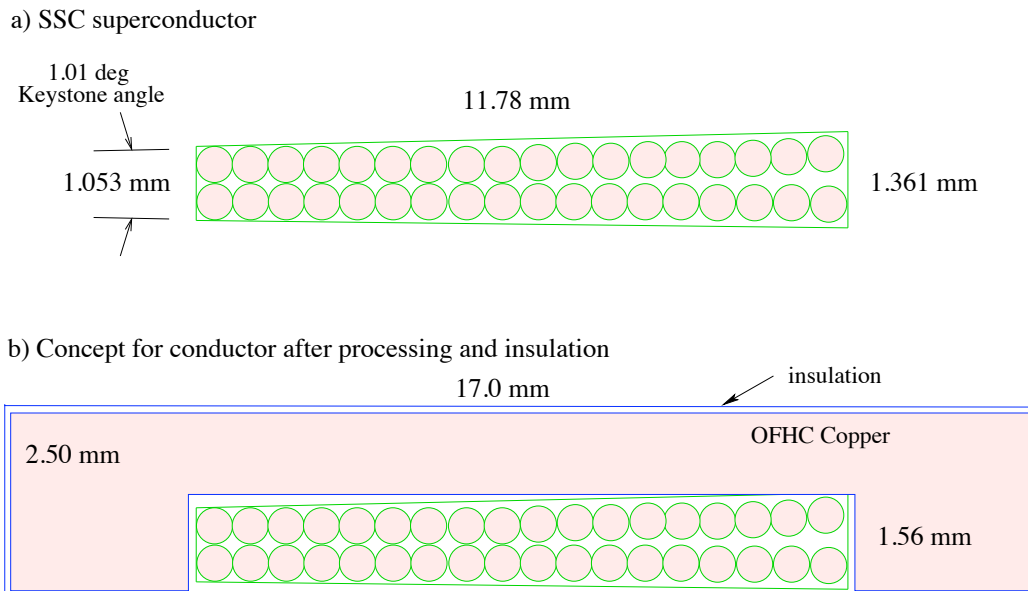


Figure 5: a) Superconductor available from JLab for potential use in the solenoid. b) Concept for composite conductor with the superconductor soldered into a copper channel substrate and insulated; typical dimensions are indicated.

References

- [1] D. Aston et al. The LASS spectrometer. SLAC-R-298. <http://www.slac.stanford.edu/pubs/slacreports/slac-r-298.html>, 1986. 1
- [2] G. Biallas, E. Chudakov, E.S. Smith, T. Whitlatch, and E. Wolin. Overview of the Hall D solenoid refurbishment and testing. GlueX-doc-1612, September 2010. 1